Seismic response control of transmission tower-line system using SMA-based TMD

Li Tian[1a], Mengyao Zhou[1b], Canxing Qiu[*2], Haiyang Pan[1c] and Kunjie Rong[1d]

[1]*School of Civil Engineering, Shandong University, Jinan 250061, Shandong, China*
[2]*Key Laboratory of Urban Security and Disaster Engineering of Ministry of Education,*
Beijing University of Technology, Beijing 100124, China

Abstract. This study proposes a new shape memory alloy-tuned mass damper (SMA-TMD) and investigates the effectiveness of this damper in reducing and controlling the vibrations of a transmission tower-line system under various seismic excitations. Based on a practical transmission line system and considering the geometric nonlinearity of this system, the finite element (FE) software ANSYS is used to create an FE model of the transmission tower-line system and simulate the proposed SMA-TMD. Additionally, the parameters of the SMA springs are optimized. The effectiveness of a conventional TMD and the proposed SMA-TMD in reducing and controlling the vibrations of the transmission tower-line system under seismic excitations is investigated. Moreover, the effects of the ground motion intensity and frequency ratio on the reduction ratio (η) of the SMA-TMD are studied. The vibration reduction effect of the SMA-TMD under various seismic excitations is superior to that of the conventional TMD. Changes in the ground motion intensity and frequency ratio have a significant impact on the η of the SMA-TMD. As the ground motion intensity and frequency ratio increase, the η values of the SMA-TMD first increase and then decrease. Studying the vibration reduction effects of the SMA-TMD can provide a reference for the practical engineering application of this damper.

Keywords: transmission tower-line system; shape memory alloy; tuned mass damper; vibration reduction and control; seismic excitation

1. Introduction

Rapid modern social and economic development and scientific and technological advancement are accompanied by increasing demand for the interconnection of power networks. A reliable power supply and safely operating power systems are essential for guaranteeing the daily work and saving lives of people. Transmission systems, which include transmission towers and lines, are important lifeline structures that provide modern life with a continuous energy supply. Transmission towers are a type of lattice tower that supports overhead transmission lines. Compared with conventional building structures, transmission towers are large-span tall structures with a high flexibility. They are dynamically coupled with transmission lines. The transmission tower design scheme employed at present considers only the effects of static loads, impact loads from line breaks and wind loads. However, the failure and collapse of transmission towers have been frequently reported in past severe earthquakes. For example, the 1994 Northridge earthquake caused two large transmission

towers to fail completely and interrupted the multiloop power supply (Hall 1994). The 1999 Chi-Chi earthquake caused serious damage to transmission towers (NCREE 1999). Another earthquake in 1999 struck the Duzce region of Turkey and damaged a large number of transmission towers (Erdogan *et al.* 2016). Additionally, the Wenchuan earthquake in 2008 caused severe damage to power facilities and destroyed transmission towers of various voltage classes, resulting in huge economic losses (Xie and Zhu 2011). In recent years, transmission lines have been continuously upgraded, and their transmission capacities and voltage classes have been improved; the application of new materials and technologies has led to higher tower with larger spans. As a result, seismic loading has a greater risk to severely damage transmission tower-line systems, compared with earlier cases. Therefore, research on controlling the seismic vibration of transmission tower-line systems is of great importance for improving the safety and reliability of these systems under earthquakes.

Transmission tower-line systems are highly flexible structures with a large span and low damping. Dynamic loads cause transmission tower-line systems to undergo intense unfavorable vibrations, which can potentially lead to their collapse and failure. Researchers have extensively studied the responses of transmission tower-line systems under seismic loading. Simplified and alternative models were proposed in theoretical studies (Ozono and Maeda 1992, Li *et al.* 2005) to investigate the influence of the dynamic coupling effect of transmission lines on the seismic responses of transmission tower-line systems. In

---

∗Corresponding author, Professor
 E-mail: qiucanxing@bjut.edu.cn
[a] Professor
[b] M.D. Student
[c] M.D. Student
[d] M.D. Student

Fig. 1 Photograph of a transmission tower

Fig. 2 Planar schematic of the transmission tower (mm)

Table 1 Specifications and performance indexes of the conductors and ground wires

Type	Conductors	Ground wires
Transmission line type	LGJ-400/35	LGJ-95/55
Outer diameter (m)	26.82E-3	16.00E-3
Cross-sectional area (m^2)	425.24E-6	152.81E-6
Elastic modulus (GPa)	65.00	105.00
Mass per unit length (kg/m)	1.3490	0.6967
Coefficient of linear expansion (1/°C)	2.05E-5	1.55E-5

addition, numerical simulation studies were applied to investigate the seismic responses of transmission tower-line systems (Tian *et al.* 2017a, 2018a, 2019a, 2019b, Wu *et al.* 2014); these investigations performed fragility analyses based on the probabilistic seismic demand model and presented the near-fault ground motions and angles of incidence of the seismic responses of transmission tower. Furthermore, shaking table tests were conducted to investigate the collapse failure subjected to extremely severe earthquakes and the influences of seismic spatial variations and multi-component ground motions on the dynamic responses of transmission tower-line systems (Tian *et al.* 2016, 2017b, 2018b, 2019c).

Researchers have proposed various methods to reduce these structural vibrational responses. Wu and Yang (1998) installed an active mass driver on the upper observation deck of the 310 m Nanjing TV transmission tower in China to reduce its acceleration response under strong wind gusts. Zhang (2014) and Xu *et al.* (2014a) also designed a pair of active mass driver systems and proved the AMD control effectiveness on suppressing the responses of the Canton Tower under wind excitations (Xu *et al.* 2014b). Battista *et al.* (2003) developed a nonlinear pendulum-like damper (NLPD) to reduce the wind-induced vibration of a transmission tower. To upgrade the wind-resistant
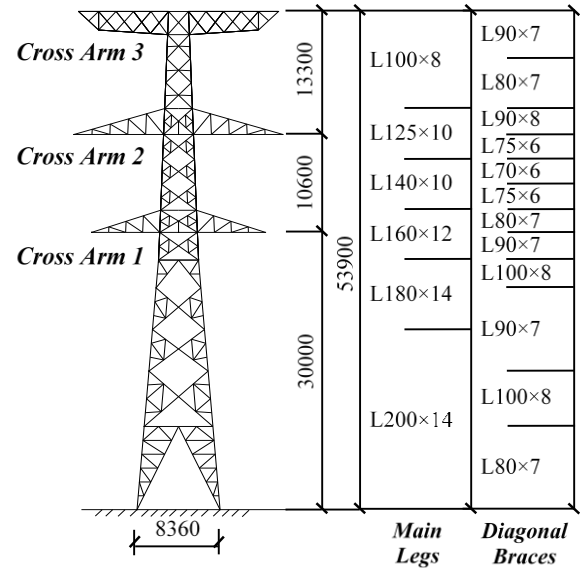
performance of a transmission tower, Park *et al.* (2007) proposed two types of friction-type reinforcing members (FRMs) that were verified through cyclic loading tests. Liu and Li (2008) proposed a method to simulate a tuned mass damper (TMD) by combining a linear spring model with the Maxwell model; their method was further adopted to calculate the wind-induced dynamic responses of a single tower and tower-line systems. Chen *et al.* (2009) proposed a magnetorheological (MR) damper to control the wind-induced responses of transmission tower-line systems. Zhang *et al.* (2015) proposed controlling the wind-induced vibration of transmission tower-line systems using spring pendulums by taking advantage of their internal resonance properties and found that spring pendulums could reduce vibrations more effectively than suspended mass pendulums. Most research is focused primarily on reducing the vibration of transmission tower-line systems under wind loads, whereas relatively few studies focused on reducing their vibration under seismic loading. Based on a TMD, Zhai *et al.* (2012) studied the vibration control schemes of transmission tower-line systems subjected to seismic ground motions, and compared the controlled system with the systems without control. To enhance the damping effect, the PTMD was used to improve the seismic-resistant performance of a transmission tower (Zhang *et al.* 2013), and the influences of the mass ratio, ground motion intensity, gap, and incident angle of the seismic ground motion were investigated (Tian *et al.* 2017c, 2019e). Further, the aforementioned ordinary linear vibration reduction and control systems are not able to dissipate seismic energy; therefore, these systems have limited vibration reduction capacities.

For this reason, the shape memory alloys (SMAs) were introduced into dampers as well as reinforced elements or joints to reduce the vibration responses of different structures subjected to ground motions (Rustighi *et al.* 2004, Sun 2011, Mishra *et al.* 2013, Torra *et al.* 2013, Fang *et al.* 2015, Jamalpour *et al.* 2017, Shiravand *et al.* 2017,
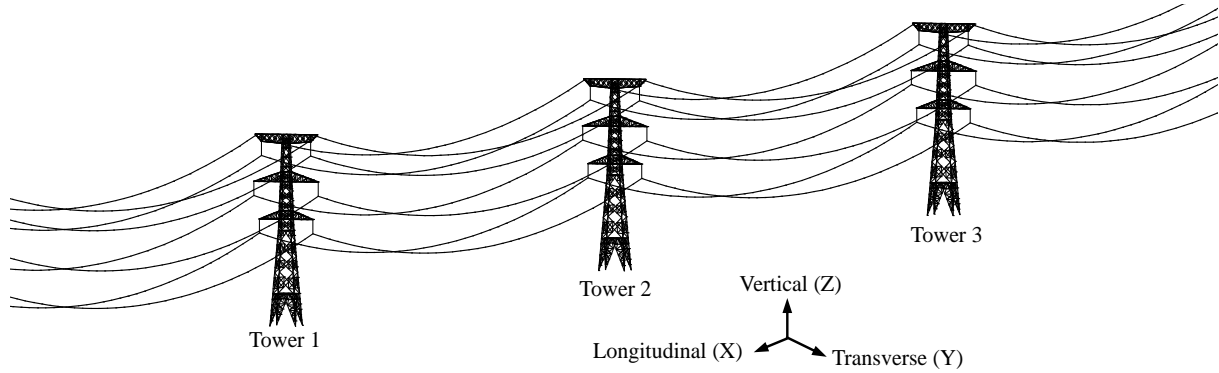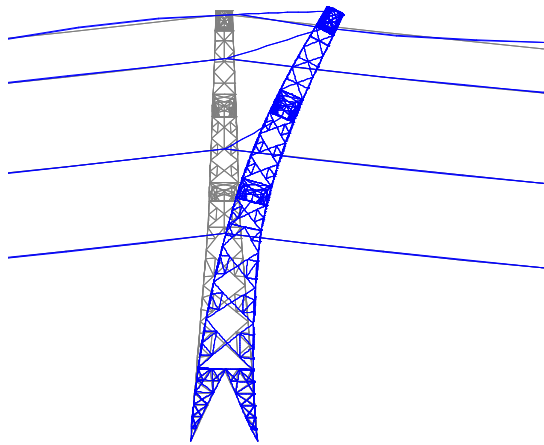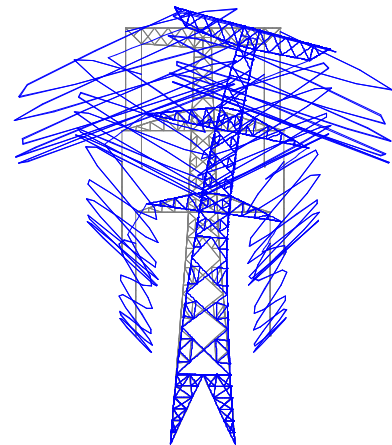
Fig. 3 Three-dimensional finite element model of transmission tower-line coupled system

(a) Longitudinal direction (b) Transverse direction

Fig. 4 Vibration mode shapes of the transmission tower-line system

Qiu and Zhu 2017a, 2017b, Qiu *et al.* 2018, Preciado *et al.* 2018, Qiu and Du 2019). Consequently, these dampers inherit the excellent self-centering properties of the SMA, and high damping mechanism. However, the applications of dampers using SMA to control the vibration of transmission tower-line systems under earthquake loadings are quite limited. To fill the research gap, this study presents a new smart TMD using conventional TMDs in combination with SMA springs. A 500 kV transmission tower-line coupled system is selected as the example. The finite element (FE) software ANSYS is used to construct a three-dimensional (3D) FE model of the transmission tower-line system and the shape memory alloy-tuned mass damper (SMA-TMD). Additionally, the parameters of the SMA springs areoptimized, and the vibration reduction effects of the SMA-TMD on the transmission tower-line system are analyzed under different natural seismic excitations. Furthermore, the effects of the ground motion intensity and frequency ratio on the vibration reduction performance of the SMA-TMD are evaluated.

2. FE model of a transmission tower-line system

This study is conducted on the basis of a typical actual 500 kV transmission line system in Northeast China. The transmission tower-line system includes transmission
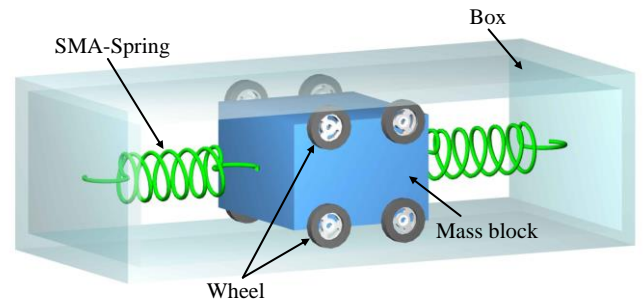

Fig. 5 Schematic of the proposed SMA-TMD

towers and transmission lines with the equal span of 400 m. Fig. 1 shows the photograph of a transmission tower, and Fig. 2 shows the elevation view and height-wise dimensions of the transmission tower. The transmission tower consists of a tower body and three cross arms (denoted by cross arms 1, 2 and 3). The tower body is 53.9 m in height, and cross arms 1, 2 and 3 are 30, 40.6 and 53.9 m above the ground, respectively. The main leg and diagonal brace materials of the transmission tower are made of Q235 and Q345 angle steel with an elastic modulus of 206 GPa, respectively. Fig. 2 also shows the member sizes of the transmission tower. The transmission lines consist of two ground wires and six conductors. The ground wires are connected to the top of the transmission tower through

insulators; similarly, the conductors are connected to the three cross arms through insulators. Table 1 summarizes the parameters of the conductors and ground wires in detail.

A 3D FE model for the transmission tower-line system is built in the ANSYS FE software. Each member of the transmission tower is simulated using BEAM188 elements. The transmission lines and insulators are simulated using LINK10 and LINK8 elements, respectively. Because transmission lines are important lifeline structures, it is usually necessary to ensure that the towers and lines keep elastic during earthquakes. This means that their post-earthquake function satisfies the desired performance indexes. Therefore, it is assumed that the transmission tower-line system is elastic. Spatially, each transmission line exhibits a catenary structure. Each transmission line is divided into 100 elements, and the materials of the lines are tension only. Additionally, the initial tension and large deformation of the transmission lines are considered. Although soil-structure interactions may affect the seismic response of the transmission tower-line system (Bi *et al.* 2011), it is assumed that the bottom of the transmission tower is fixed on the ground to simplify this problem. A transmission tower-line system consists of a continuous repetition of transmission towers and lines. Based on previous research results (Tian *et al.* 2010), a three-tower four-line model is selected as the study object. Fig. 3 shows the three-tower four-line FE model. The outermost ends of each side-span transmission line are hinged at the same height on the adjacent transmission towers. It shows the longitudinal, transverse and vertical coordinate system of the transmission tower-line system. The FE model of the transmission tower-line system is analyzed to determine its dynamic properties. The first-order frequencies of the transmission tower-line system (primarily the vibration of the transmission tower) in the longitudinal and transverse directions are 1.583 and 1.497 Hz, respectively. Fig. 4 shows the corresponding vibration modes.

3. Vibration reduction mechanism of the SMA-TMD

3.1 SMA-TMD

SMA is a new type of smart material that is capable of recovering nonlinear deformation and meanwhile dissipating energy; hence, such material is being increasingly studied and applied in a number of fields. The addition of a smart material is a key technology for developing smart systems in civil engineering. Smart materials can respond to external disturbances by automatically adjusting the internal properties of the system, thereby improving its safety and maintainability and prolonging its service life (Song *et al.* 2006).

SMAs exist in two phases, namely, austenite and martensite, and SMA materials exhibit two types of transformations: temperature-induced transformations, which refers to shape memory effect (SME), and stress-induced transformations, which refers to superelastic effect (SE) (Song *et al.* 2006). Under the action of temperature, when SMA transforms from the austenite state to the
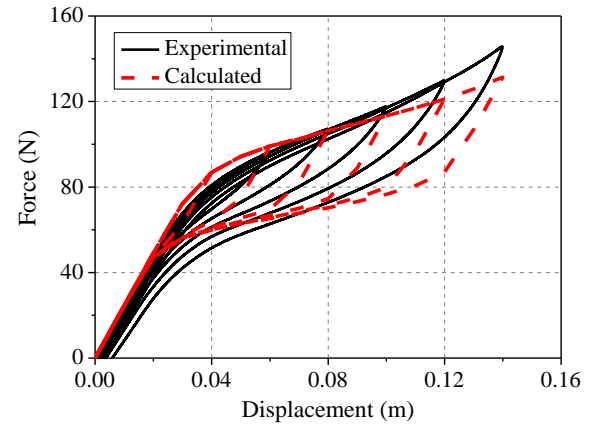

Fig. 6 Comparison between the test results and numerical simulations (Tian *et al.* 2019d; experimental data are from Qiu 2016)

martensite state and then back to the austenite state, an SME occurs. When the temperature is higher than the austenite finish temperature, the SMA that has already undergone a nonelastic strain transforms in reverse from the martensitic state to the parent phase under loading and thus recovers its original shape (Frick *et al.* 2005). This phase change results in the formation of SE hysteresis loops and provides the material an excellent fatigue resistance.

To reduce structural vibrations, a new SMA-TMD is proposed based on both the vibration reduction mechanism of a TMD and the SE of an SMA spring, as shown in Fig. 5. The SMA-TMD consists of a mass block, two SMA springs, eight pulleys and a box. It is assumed that no contact friction exists between the pulleys and the box, which is assumed frictionless. The proposed SMA-TMD has two features: (1) when the seismic load is small, the SMA springs can be treated as ordinary springs that exhibit linear behavior, and the SMA-TMD is equivalent to a conventional TMD; (2) when the seismic load is large, the forward phase change of the SMA is activated, and thus, the SMA springs enter a nonlinear stage and start to dissipate energy. Thus, the SMA-TMD combines the advantages of a conventional TMD with the hysteretic energy dissipation capacity of an SMA. The SMA springs constitute the core hysteretic energy dissipation mechanism of the SMA-TMD. Compared with a conventional TMD, the SMA-TMD has a wider vibration absorption frequency band and a higher vibration absorption efficiency.

3.2 Optimization of the SMA springs

Tian *et al.* (2019d) conducted FE simulations based on the test data obtained by Qiu *et al.* (2014) for M-CuAlBe, P-CuAlBe and NiTi alloys, and the results showed that the NiTi alloys exhibited good hysteretic behavior. In this study, NiTi alloy is selected as the material for the springs in the proposed SMA-TMD. Fig. 6 shows a comparison between the numerical simulation and experimental data for the SMA springs; clearly, the numerical model satisfactorily captures the hysteretic behavior of the SMA springs. Table 2 summarizes the parameters of the selected NiTi-based SMA at room temperature.
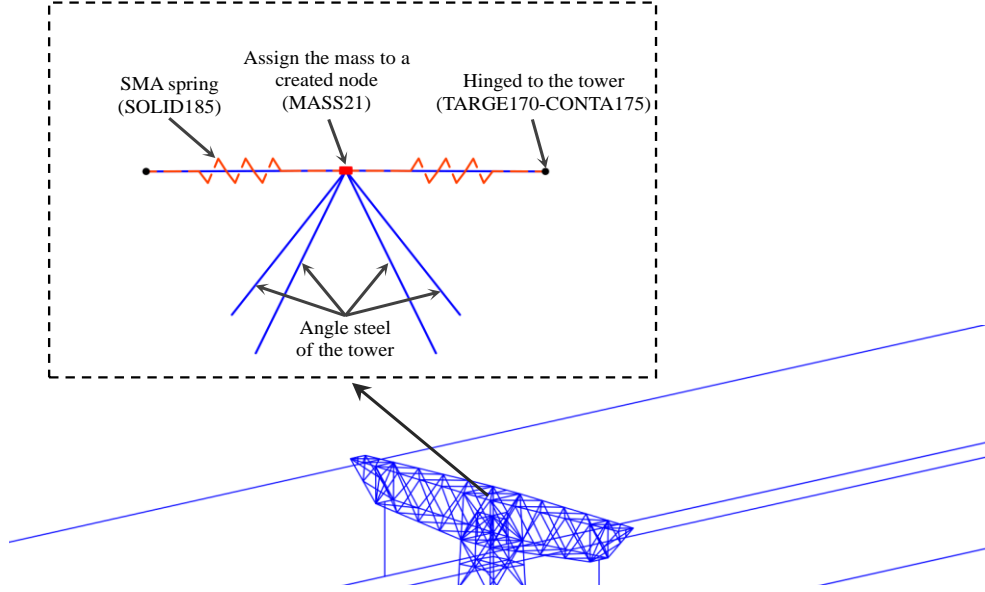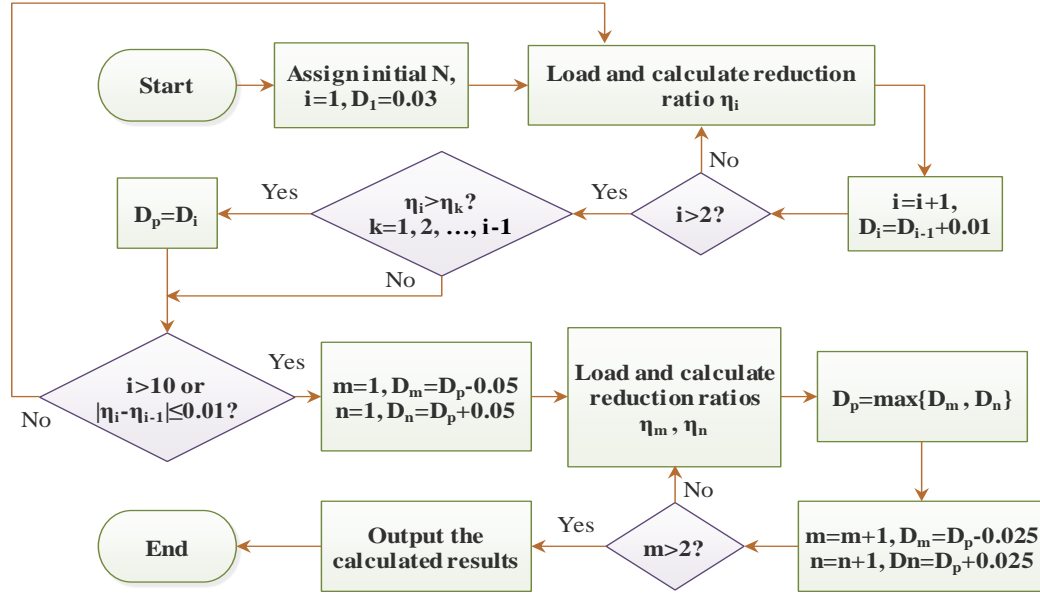
Fig. 7 Simulating the SMA-TMD in ANSYS

Fig. 8 Computational flowchart of the transmission tower-line system with different SMA springs

Table 2 Material properties of the NiTi alloy at room temperature (Tian *et al.* 2019d)

Type	E (GPa)	C1 (MPa)	C2 (MPa)	C3 (MPa)	C4 (MPa)	C5 (MPa)	C6 (MPa)
NiTi	38.3	500	600	351	300	0.04	0

Researchers have proposed a number of methods to determine the optimal control parameters of a TMD. The optimal frequency ratio proposed in reference (Den Hartog 1947) is used in this study:

$$f_{opt} = \frac{1}{1 + \mu_m} \tag{1}$$

where μ_m is the ratio of the mass of the SMA-TMD to the

corresponding modal mass of the structure (μ_m=0.02 in this study). The optimal stiffness of the SMA-TMD is as follows:

$$k_{opt} = f_{opt}^2 \omega^2 m \tag{2}$$

where m is the mass of the mass block and ω is the fundamental frequency of the structure.

The shape parameters of the SMA spring are calculated using the following equation:

$$d = \left(\frac{16 \cdot k \cdot n \cdot D^3 \cdot (1+\nu)}{E} \right)^{\frac{1}{4}} \tag{3}$$

$$t = (0.28 \sim 0.5)D \tag{4}$$

(a) Acceleration   (b) Displacement

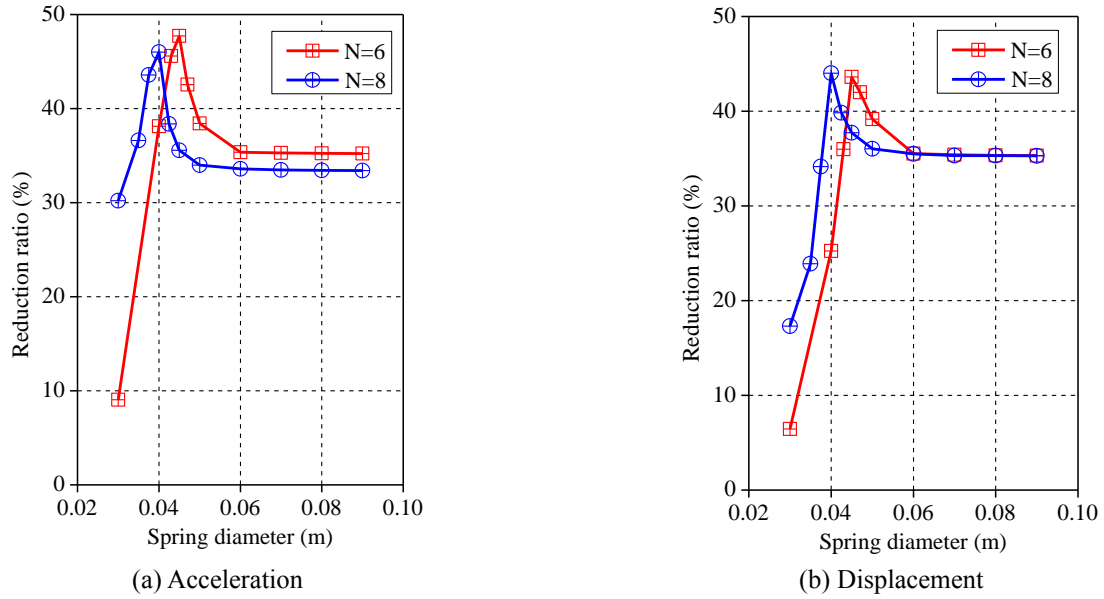Fig. 9 Variations in the reduction ratio of the transmission tower-line system with different SMA springs

Table 3 Seismic records

ID	Earthquake	Event year	Magnitude	Station
GM1	Kobe	1995	6.9	Oka
GM2	Imperial Valley	1940	6.9	El Centro
GM3	Duzce	1999	7.1	Bolu
GM4	Kern County	1952	7.4	Taft Lincoln School

where d is the wire diameter of the spring, n is the number of coils in the spring, k is the lateral stiffness of the spring, D is the pitch diameter of the spring, v is Poisson's ratio (v=0.3), E is the elastic modulus (E=38.3 GPa), and t is the pitch of the spring (t=0.4D). n, D and d are determined based on the practical situation.

To optimize the vibration reduction effect with SMA springs, SMA springs with various shapes are analyzed. Research has found that vibration reduction devices can achieve optimal vibration reduction results when the device is installed on top of the structure (Rana and Soong 1998). Thus, the SMA-TMD is installed on top of the transmission tower. In the FE simulation software ANSYS, the mass block and SMA spring are simulated by using MASS21 and SOLID185 elements, respectively. A mapped mesh is generated for the SMA spring elements. The mass block is connected to the corresponding nodes at the top of the transmission tower through SMA springs. The node-to-surface contacts between the mass block and the SMA springs and between the SMA springs and the nodes of the transmission tower are simulated by TARGE170 and CONTA175 contact elements, respectively. Fig. 7 shows the simulated SMA-TMD.

To examine the effects of the SMA spring shape, two values of n are considered, and D is set to vary between 0.02 and 0.09 m. Fig. 8 shows the computation process. The OKA-000 component record of the 1995 Kobe earthquake is selected and input along the longitudinal direction of the unchanged. Fig. 9 shows the relationship between
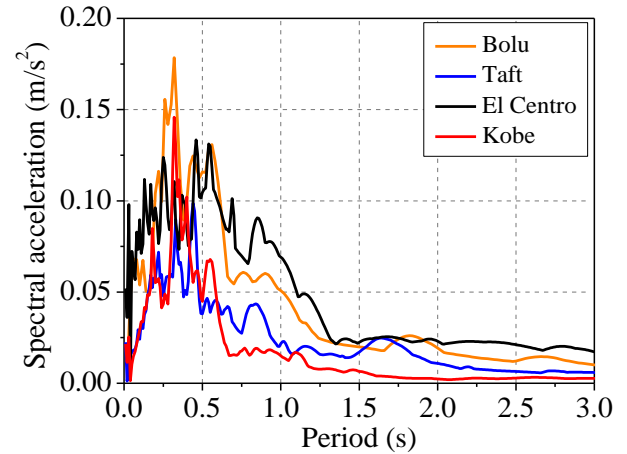

Fig. 10 Spectral accelerations of the recorded ground motions

transmission tower-line system. D is varied, while n is reduction ratio (η) and the peak acceleration and the displacement of the top of the transmission tower. For the two values of n, the peak acceleration and displacement η exhibit the similar trend as D changes. Specifically, η first increases and reaches its maximum value and then decreases and tends to stabilize as D increases. The D values corresponding to the maximum η values are smaller using n=8 than using n=6. The maximum acceleration η when n=6 is 47.73%, which is higher than that when n=8. Thus, in the subsequent analysis of the vibration reduction performance of the SMA-TMD, n and D are set to 6 and 0.045 m, respectively.

4. Vibration control analysis

4.1 Selection of seismic waves

Considering the randomness of ground motions, four natural seismic waves are selected and input along the
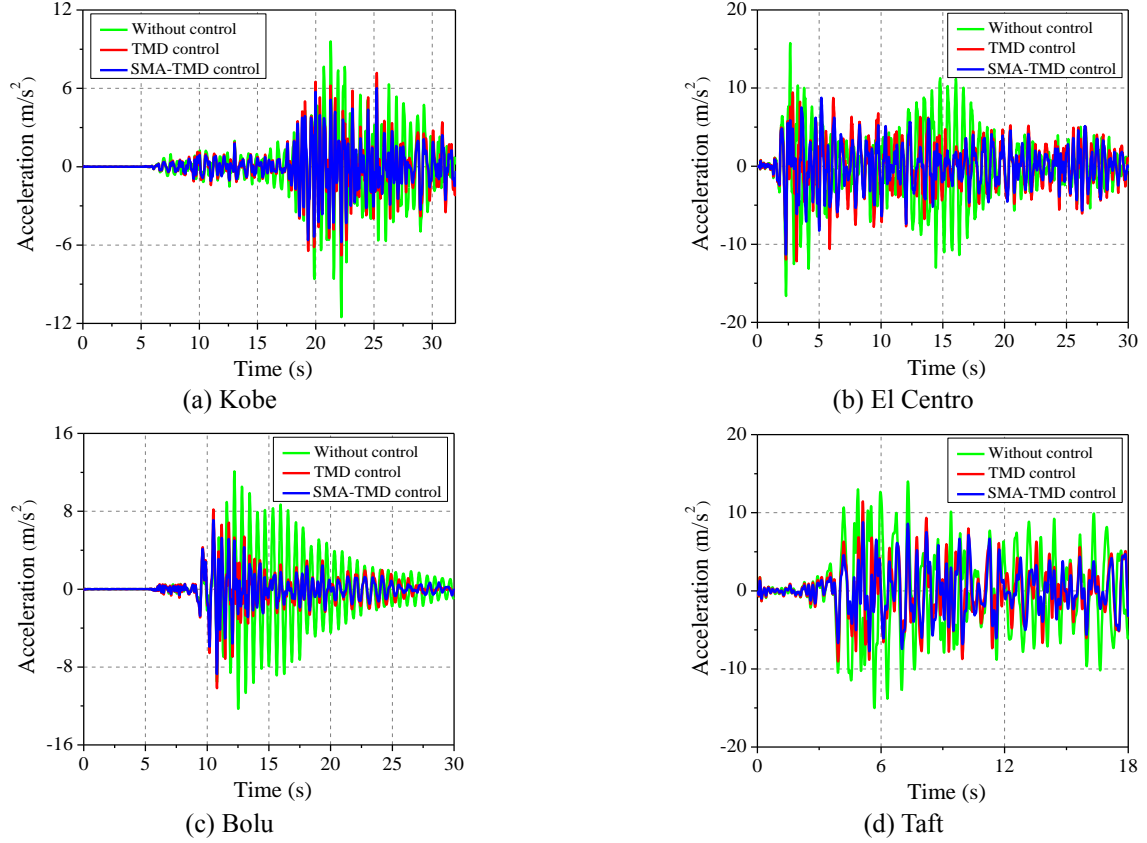
(a) Kobe   (b) El Centro

(c) Bolu   (d) Taft

Fig. 11 Acceleration responses of the transmission tower-line system under different seismic excitations

longitudinal direction of the transmission tower-line system. Table 3 summarizes the information regarding these four natural ground motion records in detail. The peak ground acceleration (PGA) is adjusted to 0.4 g. Fig. 10 shows the spectral acceleration response time history of each ground motion.

4.2 Analysis of the vibration reduction and control results

To examine the performance of the SMA-TMD, the responses of the transmission tower-line system with and without the SMA-TMD under different ground motion excitations are analyzed using the nonlinear dynamic time history method while simultaneously considering the geometric nonlinearity of the transmission lines. In addition, to investigate the differences between the SMA-TMD and conventional TMD, the response of the transmission tower-line system with a conventional TMD is also analyzed. The other parameters of the SMA-TMD and the conventional TMD are set to be the same. The only difference between the two dampers is that the hysteretic energy dissipation capacity of the SMA is not considered when using the conventional TMD, and the springs in the conventional TMD follow an elastic constitutive model. To quantify the vibration reduction results, the reduction ratios of the acceleration, displacement and axial force are defined as follows:

$$\eta_\alpha = \frac{A_0 - A_c}{A_0} \times 100\% \tag{5}$$

$$\eta_d = \frac{D_0 - D_c}{D_0} \times 100\% \tag{6}$$

$$\eta_f = \frac{F_0 - F_c}{F_0} \times 100\% \tag{7}$$

where A_0 and A_c are the peak acceleration responses at the top of the transmission tower without and with control devices, respectively. Similarly, the subscripts "0" and "c" denote the uncontrolled and controlled cases, respectively, and D and F are the peak displacement response at the top of the transmission tower and the peak axial force response of the main leg of the transmission tower, respectively.

Figs. 11-13 show the dynamic responses of the transmission tower-line system without a control, with the TMD control and with the SMA-TMD control under the four ground motion excitations described above. As demonstrated in Figs. 11-13, both the TMD and the SMA-TMD can effectively reduce the dynamic response of the transmission tower, and the vibration reduction performances of the transmission tower subjected to different ground motions vary. Obviously, the SMA-TMD can more effectively control the seismic responses than the TMD for each case. Taking the El Centro seismic wave as an example, Figs. 11(b) and 12(b) show the acceleration and displacement time history curves, respectively, of the top of the transmission tower. When the transmission tower is controlled by the TMD, η_a=26.72% and η_d=23.60%, which are smaller than those (31.99% and 27.63%,

(a) Kobe

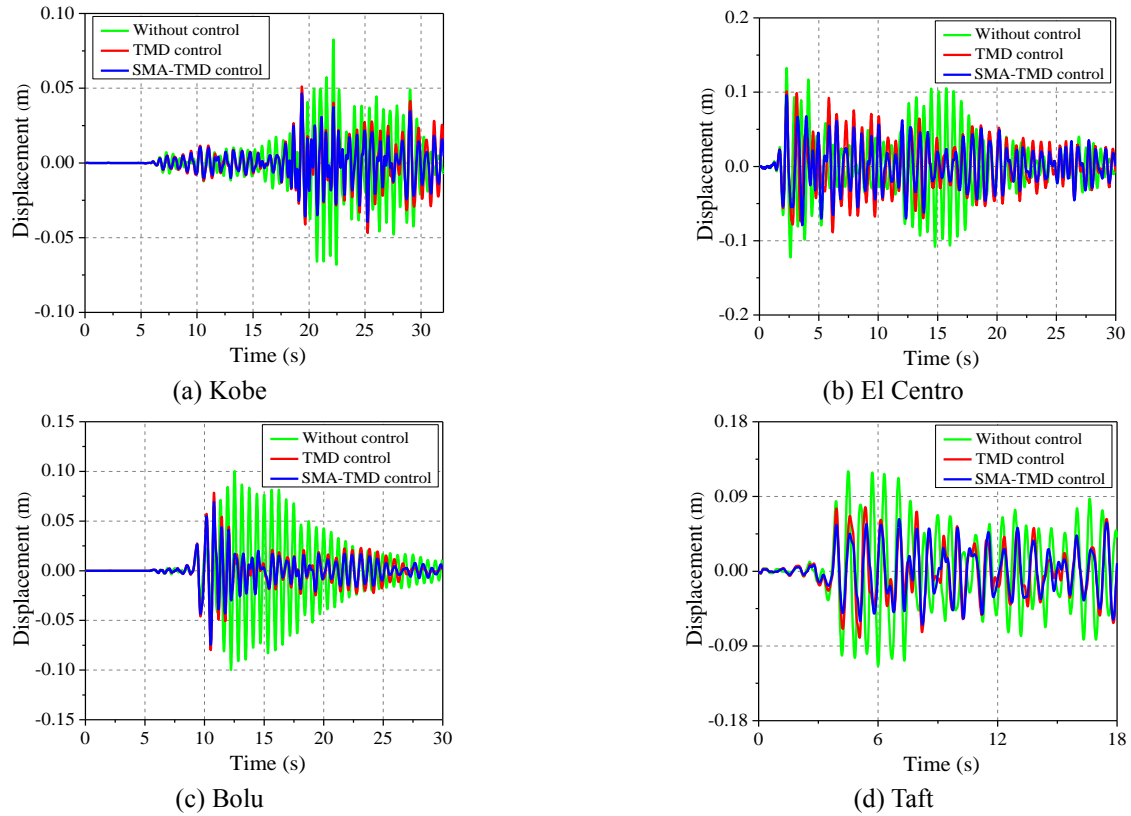(b) El Centro

(c) Bolu

(d) Taft

Fig. 12 Displacement responses of the transmission tower-line system under different seismic excitations

respectively) when the transmission tower is controlled by the SMA-TMD. Additionally, the reduction ratios of the root-mean-square (RMS) responses are better when the transmission tower is controlled by the SMA-TMD than when the transmission tower is controlled by the TMD in each case. As shown in Figs. 11(b) and 12(b), both control devices significantly reduce the response of the top of the transmission tower at 12-18 s; however, the acceleration and displacement of the top of the transmission tower may be larger when controlled by either of the control devices than the uncontrolled case, which can be explained by the energy principle of a TMD (Zhang *et al.* 2013). In other words, when the oscillation of the tower diminishes gradually, the energy is transmitted back from the TMD, which is designed to absorb kinetic energy from the primary structure, and thus, the vibrations aggregate. Fig. 13(b) shows the axial force of the main leg along the height of the transmission tower. The SMA-TMD can more effectively reduce the axial force response of the main leg of the transmission tower than the TMD. Additionally, the effects of the transmission lines and insulators at the cross arms on the reduction in the vibration of the transmission tower can be neglected.

Fig. 14 shows percentage histograms of the reduction ratios of the peak and RMS accelerations, displacements and axial forces of the transmission tower-line system under different ground motion excitations. As shown in Fig. 14, the peak and RMS values of η are better when the SMA-TMD is applied than when the TMD is applied in each case. However, the extent of the increase in each η varies with the input seismic wave. Regarding the peak η values, the SMA-

TMD shows a more significant vibration reduction than the TMD under the Taft seismic excitation. Regarding the RMS values of η, the vibration reduction with the SMA-TMD is obviously better than that with the TMD under the El Centro seismic excitation. In summary, while the η values resulting from the SMA-TMD and TMD vary under different ground motion excitations, the SMA-TMD inevitably controls the dynamic responses of the transmission tower more effectively than the TMD.

Fig. 15 shows the hysteresis curves of the SMA and ordinary springs under the four different ground motion excitations. As shown in Fig. 15, the SMA springs are capable of dissipating energy compared with the ordinary springs. The energy dissipation capacity of the SMA springs is the lowest under the Kobe seismic excitation because the predominant frequency of the Kobe seismic wave deviates significantly from the fundamental frequency of the transmission tower; as a result, the transmission tower-line system exhibits a small dynamic response, and hence, the kinetic energy of the mass block is low, and the displacement of the SMA spring is small. Nevertheless, the SMA springs have a superior energy dissipation ability under the other three earthquake loadings; the SMA springs enter a nonlinear stage and dissipate energy during the deformation process, thereby improving the vibration reduction effects of the SMA-TMD.

5. Parametric analyses

Because the recoverable phase-change process of the SMA activates its nonlinear damping behavior, the SMA-

(a) Kobe

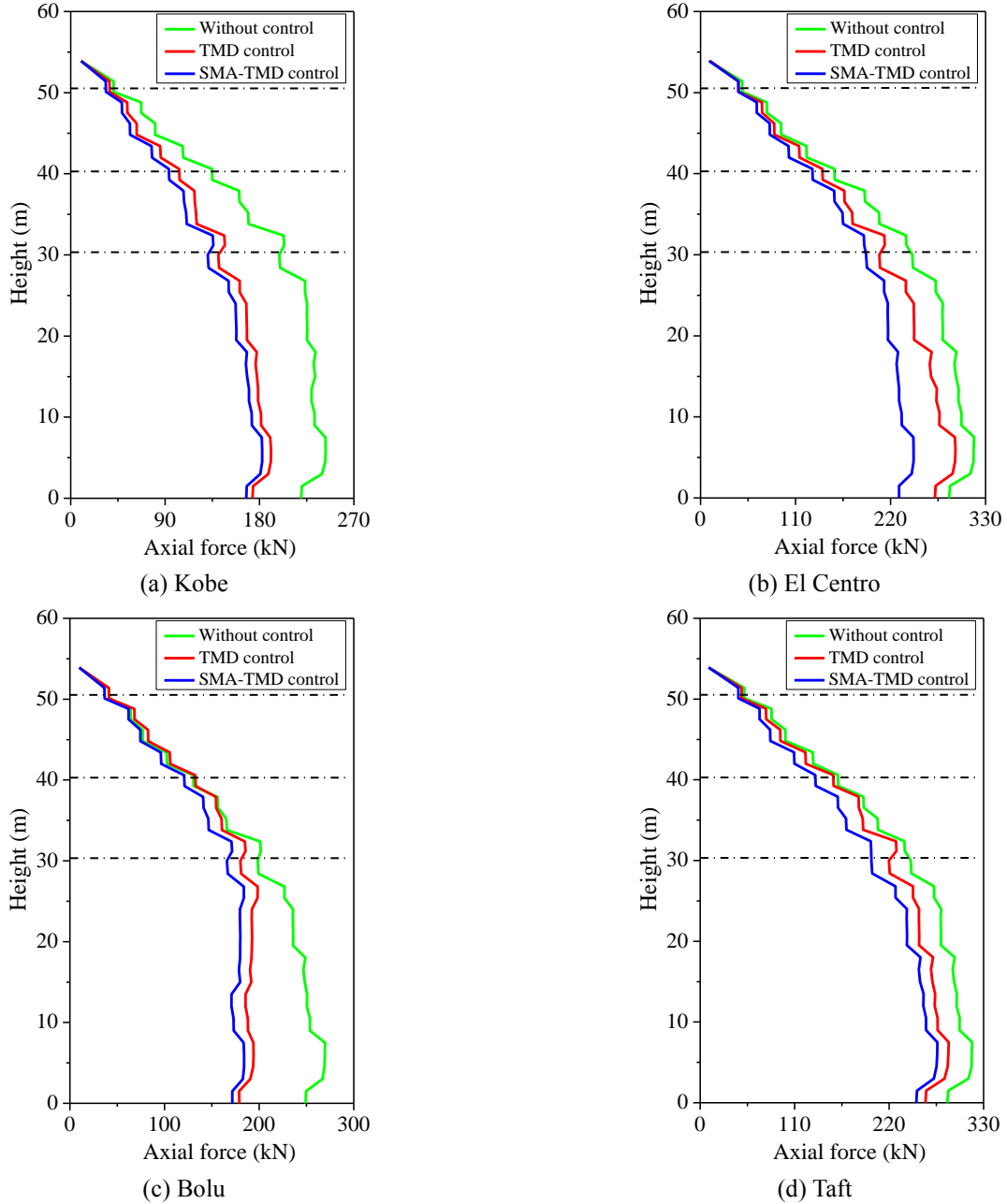(b) El Centro

(c) Bolu

(d) Taft

Fig. 13 Axial force responses of the transmission tower-line system under different seismic excitations

TMD can control the response of the structure more effectively than a conventional TMD. To further investigate the vibration reduction performance of the proposed SMA-TMD, the effects of the ground motion intensity and frequency ratio on the effectiveness of the SMA-TMD are analyzed under the El Centro earthquake loading.

5.1 Effect of the ground motion intensity

To study the effects of the ground motion intensity on the vibration reduction performance of the SMA-TMD, the effect on the SMA-TMD is analyzed under 12 PGAs ranging from 0.05 g to 0.6 g with an increment of 0.05 g while keeping the mass ratio constant at 2% and the stiffness of the SMA springs unchanged.

Fig. 16 shows the variations in the vibration reduction ratio of the SMA-TMD with different PGAs. As shown in Fig. 16, both the peak η and the RMS η resulting from the SMA-TMD first increase and reach their respective maxima at approximately 0.3 g and then start to decrease with an increase in the ground motion intensity. When the PGA is less than 0.2 g, the η values of the SMA-TMD improve slowly. This is because the SMA springs are in an elastic working stage when the ground motion intensity is small, and the force-displacement curves tend to be straight lines, which is similar to those of ordinary springs, as shown in Figs. 17(a) and (b). When the PGA exceeds 0.2 g, the deformation of each SMA spring increases, and the hysteretic behavior of the springs becomes increasingly obvious as they exhibit larger hysteresis loops. As a result
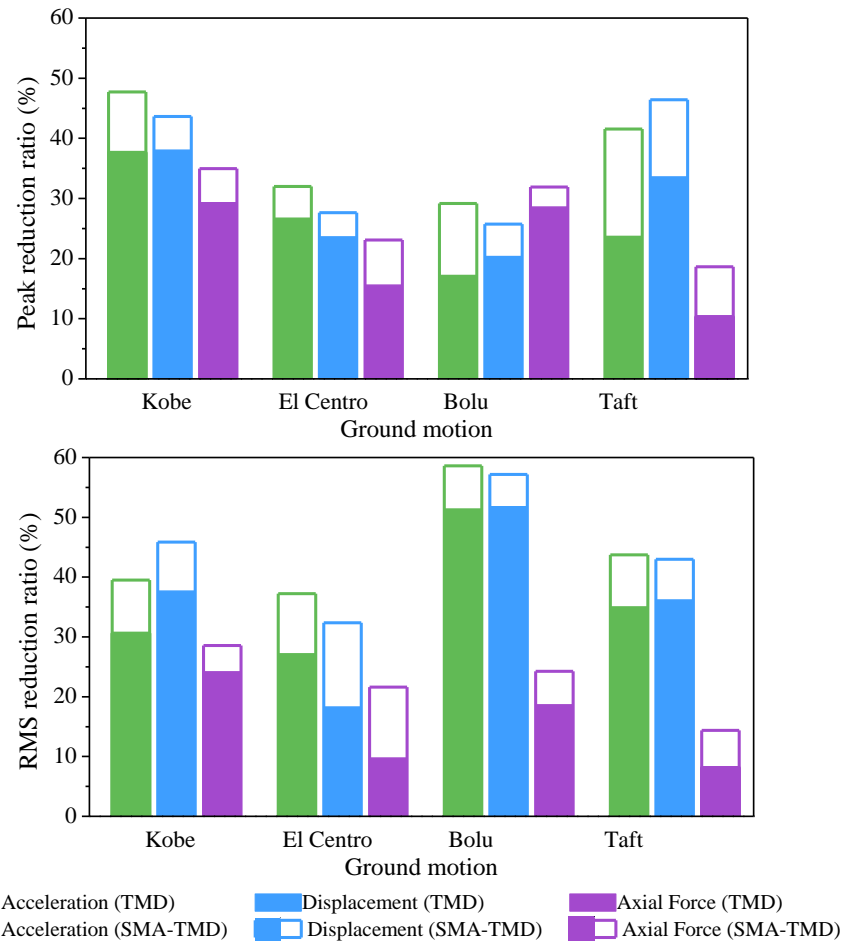
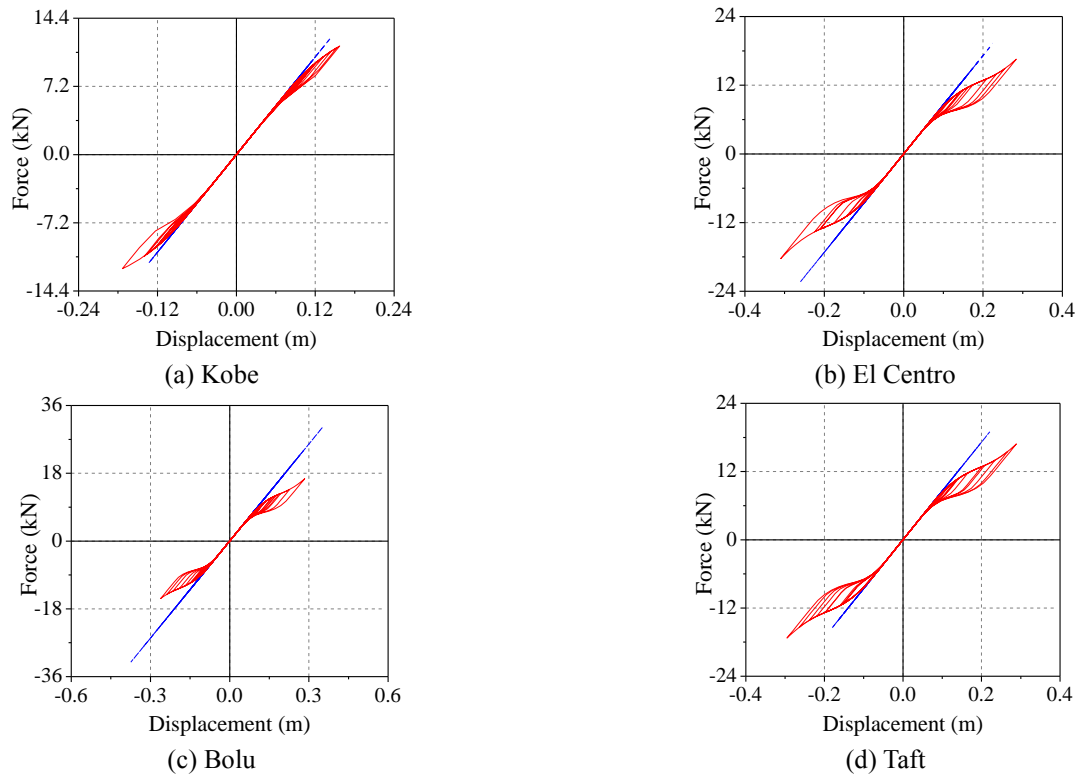Fig. 14 Vibration reduction ratios of different responses under different seismic excitations

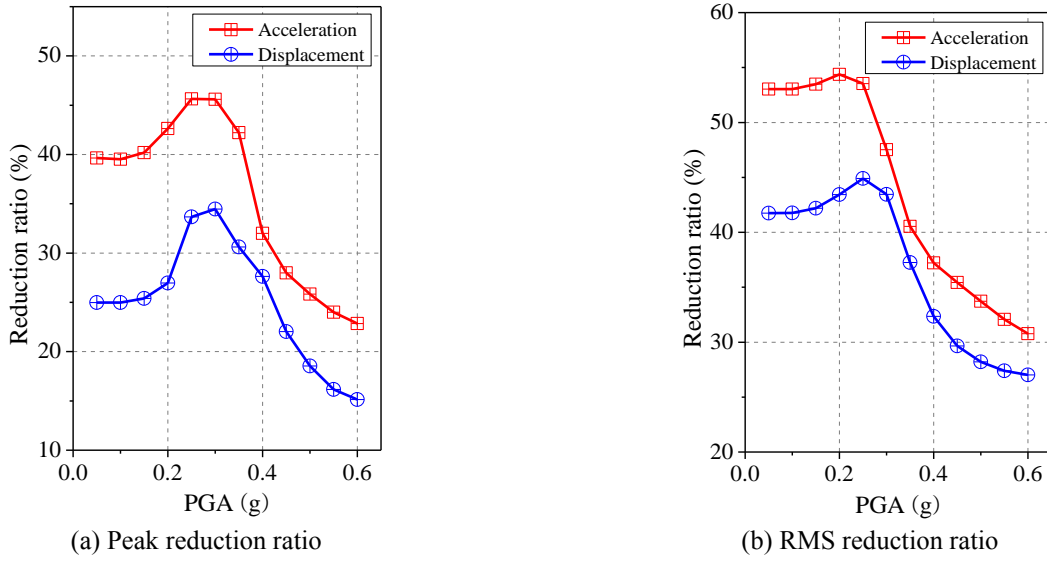Fig. 15 Hysteresis curves of the SMA and ordinary springs under different seismic excitations

(a) Peak reduction ratio

(b) RMS reduction ratio

Fig. 16 Variations in the reduction ratio of the transmission tower-line system with different PGAs

(a) PGA=0.1 g

(b) PGA=0.2 g

(c) PGA=0.3 g

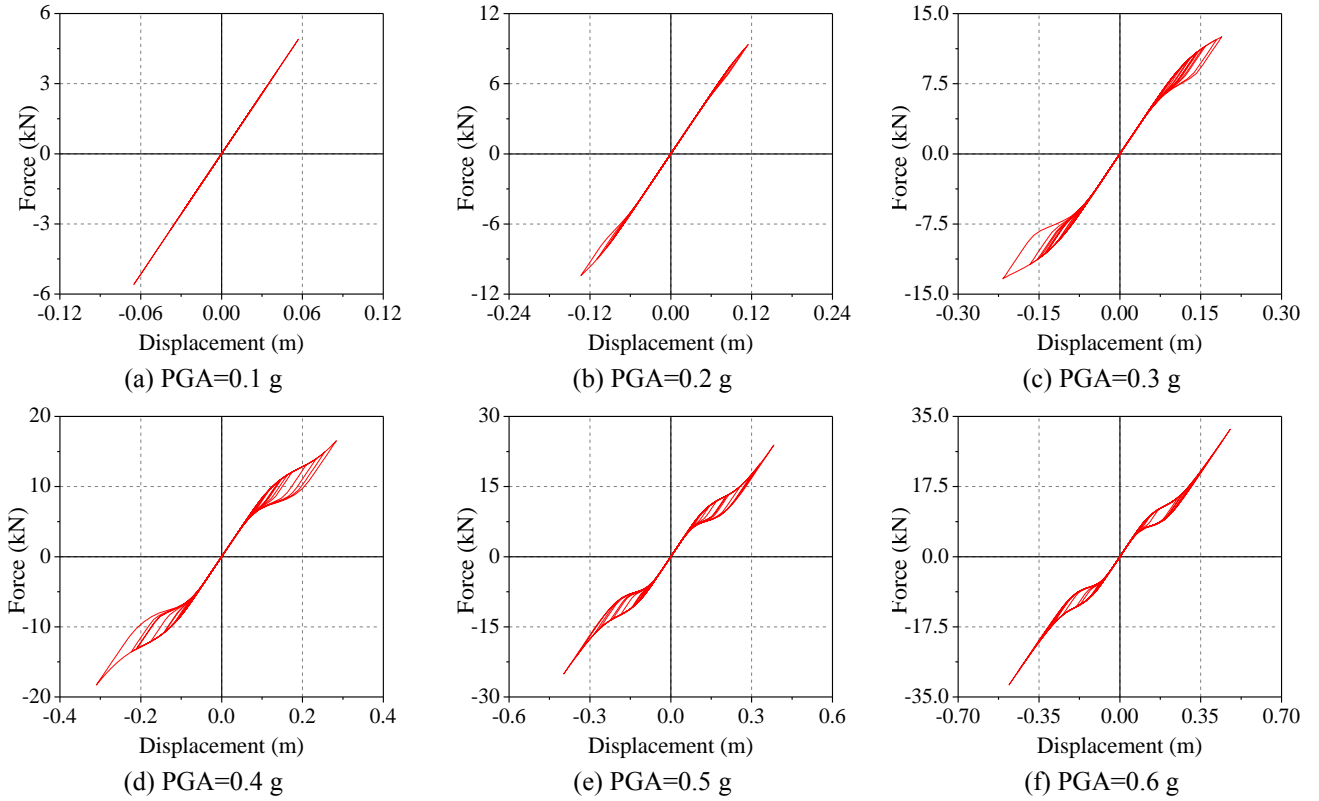(d) PGA=0.4 g

(e) PGA=0.5 g

(f) PGA=0.6 g

Fig. 17 Hysteresis curves of the SMA springs with different PGAs

of its nonlinear behavior and damping mechanism, the SMA-TMD dissipates energy while suppressing vibrations, as shown in Fig. 17(c) and (d). When the ground motion intensity continues to increase beyond 0.4 g, the hardening behavior of the SMA springs resulting from large deformation leads to a change in their performance; a strengthening stage occurs at the end of the flag-shaped hysteresis loops, and this effect becomes increasingly significant when the ground motion intensity continues to increase, as shown in Figs. 17(e) and (f). Excessive yielding results in a decrease in the energy dissipation capacity of the SMA springs; hence, the vibration reduction effects of the SMA-TMD decrease. Fig. 18 focuses on a comparison among the shapes of the hysteresis loops of the SMA springs under various PGAs and visually reveals the widening of the hysteresis loops of the SMA springs and the development of a strengthening stage with the increasing ground motion intensity.
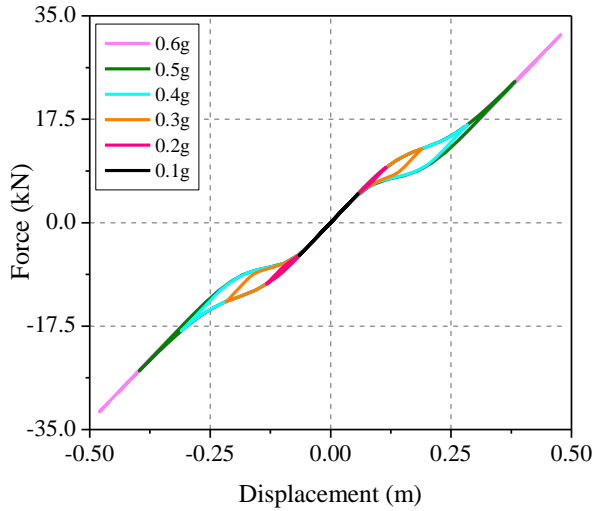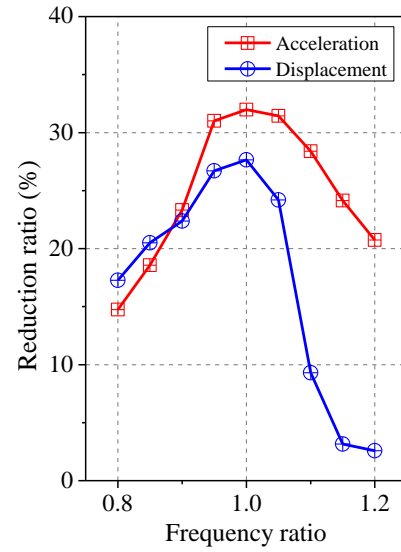
Fig. 18 Hysteresis curves of the SMA springs with different PGAs

(a) Peak reduction ratio

(b) RMS reduction ratio

Fig. 19 Variations in the reduction ratio of the transmission tower-line system with different frequency ratios
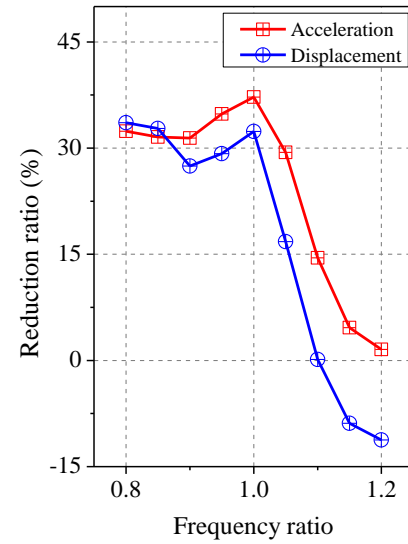
5.2 Effect of the frequency ratio

Transmission lines are exposed to natural environment. Thus, the effects of environmental factors on transmission tower-line systems cannot be ignored. Due to the strong geometric nonlinearity of transmission lines and the effects of environmental conditions (e.g., changes in temperature and ice formation), it is very difficult to accurately obtain the fundamental frequency of a transmission tower-line system in practical engineering. The natural frequencies of structures will change within a certain frequency band with variations in environmental conditions. In view of this problem, the effects of the frequency ratio varying from 0.8 to 1.2 on the vibration reduction performance of the SMA-TMD controlling the transmission tower-line system are analyzed (mass ratio=2%; PGA=0.4 g). The frequency is determined by using Equation (1). The stiffness of the SMA springs changes with the frequency ratio.

Fig. 19 shows the variations in the vibration reduction ratio of the SMA-TMD with different frequency ratios. As demonstrated in Fig. 19, the peak η values first increase and then decrease as the frequency ratio increases. Both the optimum peak and the RMS η_d values occur at a frequency ratio of 1.0. Regarding the peak values of η, the peak η_d is higher than the peak η_a when the frequency ratio is less than 0.9; the peak η_a is higher than the peak η_d when the frequency ratio is greater than 0.9; and the peak η_d decreases rapidly when the frequency ratio is greater than 1.0. Regarding the RMS η values, both the RMS η_d and the RMS η_a decrease rapidly when the frequency ratio is greater than 1.0. In particular, the RMS η_d is negative when the frequency ratio is greater than 1.1. Under this condition, the SMA-TMD amplifies the response of the structure. Fig. 20 shows the hysteretic loops of the SMA springs at various frequency ratios, and they are shown collectively in Fig. 21. As demonstrated in Figs. 20 and 21, as the frequency ratio increases, the widths of the hysteresis loops of the SMA springs first increase and then decrease. The force-displacement curve of the SMA springs is almost a straight line at a frequency ratio of 1.2. Under this condition, the

SMA-TMD displays the lowest vibration reduction effect. At a frequency ratio of 1.0, the SMA springs exhibit the widest hysteresis loops and the most notable nonlinear behavior and have the highest energy dissipation capacity. Under this condition, the SMA-TMD achieves an optimum vibration reduction effect.

6. Conclusions

This study presents a new SMA-TMD based which combines a conventional TMD and superelastic SMA springs and applies this damper to control the seismic vibrations of a transmission tower-line system. The vibration reduction effects of the SMA-TMD and a conventional TMD on the transmission tower-line system under different earthquake loadings are compared. Additionally, the effects of the ground motion intensity and

(a) Frequency ratio = 0.8

(b) Frequency ratio = 0.9

(c) Frequency ratio = 1.1

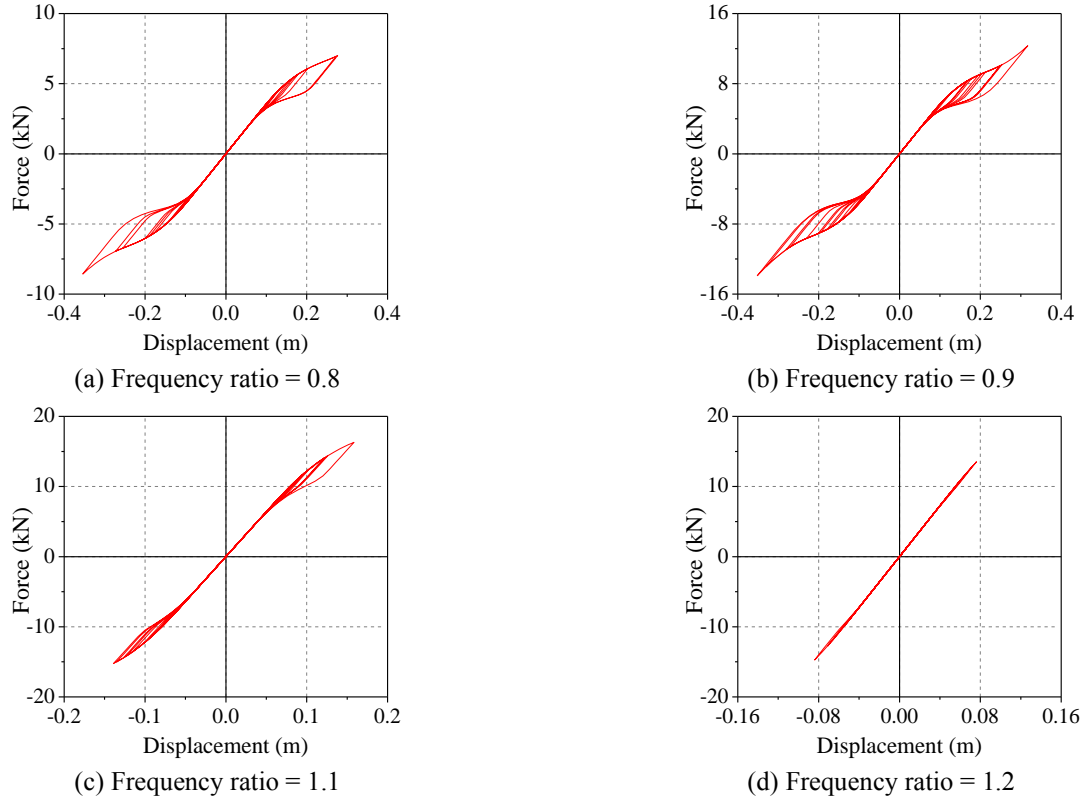(d) Frequency ratio = 1.2

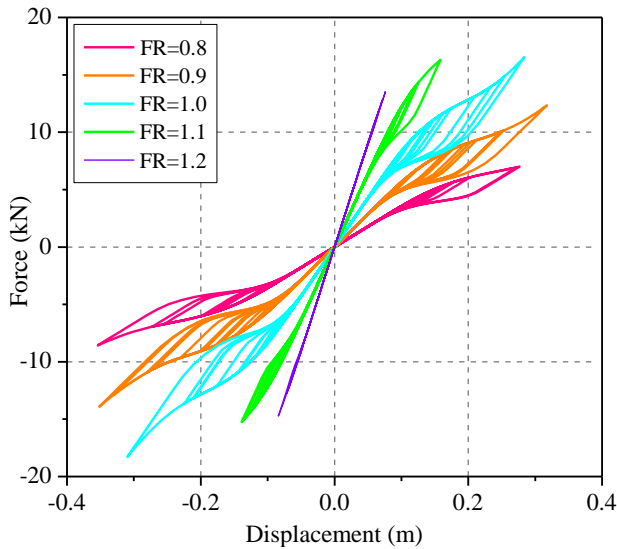Fig. 20 Hysteresis curves of the SMA springs with different frequency ratios

Fig. 21 Hysteresis curves of the SMA springs with different frequency ratios

frequency ratio on the vibration reduction capacity of the SMA-TMD are investigated. The following conclusions are derived from this study:

• When the stiffness of the SMA springs remains unchanged, their shape parameters have a great influence on the vibration reduction effect of the SMA-TMD on the transmission tower-line system. The parameters of the SMA springs should thus be optimized according to the specified structure.

• The peak and RMS η_a, η_d and η_f values of the transmission tower-line system with the SMA-TMD are better than those with a conventional TMD. This is because the SMA springs enter a nonlinear stage and are consequently capable of dissipating energy. The energy dissipation capacity of the SMA springs varies under different ground motion excitations.

• Changes in the ground motion intensity have a significant influence on the η values of the SMA-TMD. With an increasing ground motion intensity, η first increases and then decreases because the SMA springs gradually transition from an elastic working stage to a nonlinear working stage and ultimately to a hardening stage.

• Changes in the frequency ratio also have an obvious influence on the η values of the SMA-TMD. As the frequency ratio increases, η first increases and then decreases. When the frequency ratio exceeds a certain range, the η values resulting from the SMA-TMD decrease sharply; that is, the SMA-TMD amplifies the response of the structure. Therefore, selecting the appropriate frequency ratio is very important in the design of the SMA-TMD.

References

Battista, R.C., Rodrigues, R.S. and Pfeil, M.S. (2003), "Dynamic behavior and stability of transmission line towers under wind forces", *J. Wind Eng. Ind. Aerodyn.*, **91**(8), 1051-1067. https://doi.org/10.1016/s0167-6105(03)00052-7.

Bi, K., Hao, H. and Chouw, N. (2011), "Influence of ground motion spatial variation, site condition and SSI on the required separation distances of bridge structures to avoid seismic pounding", *Earthq. Eng. Struct. Dyn.*, **40**(9), 1027-1043. https://doi.org/10.1002/eqe.1076.

Buehler, W.J., Gilfrich, J.V. and Wiley, R.C. (1963), "Effect of low-temperature phase changes on the mechanical properties of alloys near composition TiNi", *J. Appl. Phys.*, **34**(5), 1475-1477. https://doi.org/10.1063/1.1729603.

Chen, B., Zheng, J. and Qu, W. (2009), "Control of wind-induced response of transmission tower-line system by using magnetorheological dampers", *Int. J. Struct. Stab. Dyn.*, **9**(04), 661-685. https://doi.org/10.1142/s0219455409003235.

Den Hartog, J.P. (1947), *Mechanical Vibrations*, (3rd Edition), McGraw-Hill, New York, NY, USA.

Erdogan, Y.S., Kocatürk, T. and Demir, C. (2016), "Seismic analysis and investigation of damage mechanism of 57th infantry regiment memorial using finite-discrete element method", *Bull. Earthq. Eng.*, **15**(4), 1397-1424. https://doi.org/10.1007/s10518-016-0024-3.

Fang, C., Yam, M. C., Lam, A. C., and Zhang, Y. (2015). "Feasibility study of shape memory alloy ring spring systems for self-centring seismic resisting devices", *Smart Mater. Struct.*, **24**(7), https://doi.org/10.1088/0964-1726/24/7/075024.

Frick, C.P., Ortega, A.M., Tyber, J., Maksound, A.E.M., Maier, H.J., Liu, Y. and Gall, K. (2005), "Thermal processing of polycrystalline NiTi shape memory alloys", *Mater. Sci. Eng. A-Struct. Mater. Prop. Microstruct. Process.*, **405**(1-2), 34-49. https://doi.org/10.1557/proc-855-w1.9.

Hall, J.F., Holmes, W. and Somers, P. (1994), "Northridge Earthquake, January 17, 1994", Preliminary Reconnaissance Report.

Jamalpour, R., Nekooei, M. and Moghadam, A. S. (2017). "Seismic behavior of steel column-base-connection equipped by NiTi shape memory alloy", *Struct. Eng. Mech.*, **64**(1), 109-120. http://dx.doi.org/10.12989/sem.2017.64.1.109.

Li, H.N., Shi, W.L., Wang, G.X. and Jia, L.G. (2005), "Simplified models and experimental verification for coupled transmission tower–line system to seismic excitations", *J. Sound Vibr.*, **286**(3), 569-585. https://doi.org/10.1016/j.jsv.2004.10.009.

Liu, G.H. and Li, H.N. (2008), "Analysis and optimization control of wind-induced dynamic response for high-voltage transmission tower-line system", *Proc. Chin. Soc. Elec. Eng.*, **28**(19), 131-137. https://doi.org/10.13334/j.0258-8013.pcsee.2008.19.013.

Mishra, S.K., Gur, S. and Chakraborty, S. (2013), "An improved tuned mass damper (SMA-TMD) assisted by a shape memory alloy spring", *Smart Mater. Struct.*, **22**(9), 095016. https://doi.org/10.1088/0964-1726/22/9/095016.

NCREE (1999), "Damage report on 921 Chi-Chi earthquake-lifeline system", National Center for Research on Earthquake Engineering.

Ozono, S. and Maeda, J. (1992), "In-plane dynamic interaction between a tower and conductors at lower frequencies", *Eng. Struct.*, **14**(4), 210-216. https://doi.org/10.1016/0141-0296(92)90009-f.

Park, J.H., Moon, B.W., Min, K.W., Lee, S.K. and Kim, C.K. (2007), "Cyclic loading test of friction-type reinforcing members upgrading wind-resistant performance of transmission towers", *Eng. Struct.*, **29**(11), 3185-3196. https://doi.org/10.1016/j.engstruct.2007.03.022.

Preciado, A., Ramirez-Gaytan, A., Gutierrez, N., Vargas, D., Falcon, J. M. and Ochoa, G. (2018). "Nonlinear earthquake capacity of slender old masonry structures prestressed with steel, FRP and NiTi SMA tendons", *Steel Compos. Struct.*, **26**(2), 213-226. http://dx.doi.org/10.12989/scs.2018.26.2.213.

Qiu, C. and Zhu, S. (2014), "Characterization of cyclic properties of superelastic monocrystalline Cu–Al–Be SMA wires for seismic applications", *Constr. Build. Mater.*, **72**, 219-230. https://doi.org/10.1016/j.conbuildmat.2014.08.065.

Qiu, C. (2016). "Seismic-resisting self-centering structures with superelastic shape memory alloy damping devices", Ph.D. Dissertation, The Hong Kong Polytechnic University, Hong Kong.

Qiu, C., and Zhu, S. (2017a). "Shake table test and numerical study of self-centering steel frame with SMA braces", *Earthq. Eng. Struct. Dyn.*, **46**(1), 117-137. https://doi.org/10.1002/eqe.2777.

Qiu, C., and Zhu, S. (2017b). "Performance-based seismic design of self-centering steel frames with SMA-based braces", Eng. Struct., **130**, 67-82. https://doi.org/10.1016/j.engstruct.2016.09.051.

Qiu, C., Zhang, Y., Qi, J. and Li, H. (2018). "Seismic behavior of properly designed CBFs equipped with NiTi SMA braces", *Smart. Struct. Syst.*, **21**(4), 479-491. http://dx.doi.org/10.12989/sss.2018.21.4.479.

Qiu, C., and Du X.L. (2019). "Seismic performance of multistory CBFs with novel recentering energy dissipative braces", *J. Constr. Steel. Res.*, 105864. https://doi.org/10.1016/j.jcsr.2019.105864.

Rana, R. and Soong, T.T. (1998), "Parametric study and simplified design of tuned mass dampers", *Eng. Struct.*, **20**(3), 193-204. https://doi.org/10.1016/s0141-0296(97)00078-3.

Rustighi, E., Brennan, M.J. and Mace, B.R. (2004), "A shape memory alloy adaptive tuned vibration absorber: design and implementation", *Smart Mater. Struct.*, **14**(1), 19. https://doi.org/10.1088/0964-1726/14/1/002.

Shiravand, M. R., Khorrami Nejad, A. and Bayanifar, M. H. (2017). "Seismic response of RC structures rehabilitated with SMA under near-field earthquakes", *Struct. Eng. Mech.*, **63**(4), 497-507. http://dx.doi.org/10.12989/sem.2017.63.4.497.

Song, G., Ma, N. and Li, H.N. (2006), "Applications of shape memory alloys in civil structures", *Eng. Struct.*, **28**(9), 1266-1274. https://doi.org/10.1016/j.engstruct.2005.12.010.

Sun, W. (2011), "Seismic response control of high arch dams including contraction joint using nonlinear super-elastic SMA damper", *Constr. Build. Mater.*, **25**(9), 3762-3767. https://doi.org/10.1016/j.conbuildmat.2011.04.013.

Tian, L., Li, H. and Liu, G. (2010), "Seismic Response of Power Transmission Tower-Line System Subjected to Spatially Varying Ground Motions", *Math. Probl. Eng.*, **2010**, 1–20. https://doi.org/10.1155/2010/587317.

Tian, L., Gai, X., Qu, B., Li, H. and Zhang, P. (2016), "Influence of spatial variation of ground motions on dynamic responses of supporting towers of overhead electricity transmission systems: An experimental study." *Eng. Struct.*, **128**, 67-81. https://doi.org/10.1016/j.engstruct.2016.09.010.

Tian, L., Pan, H., Ma, R. and Qiu, C. (2017a). "Collapse simulations of a long span transmission tower-line system subjected to near-fault ground motions", *Earthq. Struct.*, **13**(2), 211-220. https://doi.org/10.12989/eas.2017.13.2.211.

Tian, L., Gai, X. and Qu, B. (2017b), "Shake table tests of steel towers supporting extremely long-span electricity transmission lines under spatially correlated ground motions", *Eng. Struct.*, **132**, 791-807. https://doi.org/10.1016/j.engstruct.2016.11.068.

Tian, L., Rong, K., Zhang, P. and Liu, Y. (2017c), "Vibration control of a power transmission tower with pounding tuned mass damper under multi-component seismic excitations", *Appl. Sci.-Basel*, **7**(5), 477. https://doi.org/10.3390/app7050477.

Tian, L., Yi, S. and Qu, B. (2018a), "Orienting Ground Motion

Inputs to Achieve Maximum Seismic Displacement Demands on Electricity Transmission Towers in Near-Fault Regions", *J. Struct. Eng.*, **144**(4), 04018017. https://doi.org/10.1061/(asce)st.1943-541x.0002000.

Tian, L., Ma, R., Qiu, C., Xin, A., Pan, H. and Guo, W. (2018b). "Influence of multi-component ground motions on seismic responses of long-span transmission tower-line system: An experimental study", *Earthq. Struct.*, **15**(6), 583-593. https://doi.org/10.12989/eas.2018.15.6.583.

Tian, L., Pan, H. and Ma, R. (2019a), "Probabilistic seismic demand model and fragility analysis of transmission tower subjected to near-field ground motions", *J. Constr. Steel. Res.*, **156**, 266-275. https://doi.org/10.1016/j.jcsr.2019.02.011.

Tian, L., Pan, H., Ma. R., and Dong, X. (2019b), "Seismic failure analysis and safety assessment of an extremely long-span transmission tower-line", *Struct. Eng. Mech.*, **71**(3), 305-315. https://doi.org/10.12989/sem.2019.71.3.305.

Tian, L., Fu, Z., Pan, H., Ma, R. and Liu, Y. (2019c). "Experimental and numerical study on the collapse failure of long-span transmission tower-line systems subjected to extremely severe earthquakes", *Earthq. Struct.*, **16**(5), 513-522. https://doi.org/10.12989/eas.2019.16.5.513.

Tian, L., Gao, G., Qiu, C. and Rong, K. (2019d), "Effect of hysteresis properties of shape memory alloy-tuned mass damper on seismic control of power transmission tower", *Adv. Struct. Eng.*, **22**(4), 1007-1017. https://doi.org/10.1177/1369433218791606.

Tian, L., Rong, K., Bi, K. and Zhang, P. (2019e), "A bidirectional pounding tuned mass damper and its application to transmission tower-line system under seismic excitations", *Int. J. Struct. Stab. Dy.*, **19**(6), 1950056. https://doi.org/10.1142/s0219455419500561.

Torra, V., Auguet, C., Isalgue, A., Carreras, G., Terriault, P. and Lovey, F.C. (2013), "Built in dampers for stayed cables in bridges via SMA. The SMARTeR-ESF project: a mesoscopic and macroscopic experimental analysis with numerical simulations", *Eng. Struct.*, **49**, 43-57. https://doi.org/10.1016/j.engstruct.2012.11.011.

Wu, G., Zhai, C., Li, S. and Xie, L. (2014), "Effects of near-fault ground motions and equivalent pulses on Large Crossing Transmission Tower-line System", *Eng. Struct.*, **77**, 161-169. https://doi.org/10.1016/j.engstruct.2014.08.013.

Wu, J.C. and Yang, J.N. (1998), "Active control of transmission tower under stochastic wind", *J. Struct. Eng.*, **124**(11), 1302-1312. https://doi.org/10.1109/acc.1997.609653.

Xie, Q. and Zhu, R. (2011), "Earth, wind, and ice", *IEEE Power Energy Mag.*, **9**(2), 28-36. https://doi.org/10.1109/mpe.2010.939947.

Xu, H.B., Zhang, C.W., Li, H. and Ou, J.P. (2014a), "Real-time hybrid simulation-based performance verification of an active mass driver (AMD) driven by a linear motor", *Struct. Control Hlth.*, **21**(4), 574–589. https://doi.org/10.1002/stc.1585.

Xu, H.B., Zhang, C.W., Li, H., Tan, P., Ou, J.P. and Zhou, F.L. (2014b), "Active mass driver control system for suppressing wind induced vibration of the Canton Tower structure", *Smart Struct. Syst.*, **13**(2), 281-303. https://doi.org/10.12989/sss.2014.13.2.281.

Zhai, C.H., Wu, G., Li, S. and Xie, L. L. (2012), "Tower-lines in-plane coupling and TMD seismic control of large crossing transmission tower lines system", *J. Vib. Eng.*, **25**(4), 431-438. https://doi.org/10.16385/j.cnki.issn.1004-4523.2012.04.018.

Zhang, C. (2014), "Control force characteristics of different control strategies for the wind-excited 76-story benchmark building structure", *Adv. Struct. Eng.*, **17**(4), 543-559. https://doi.org/10.1260/1369-4332.17.4.543.

Zhang, P., Song, G., Li, H.N. and Lin, Y. X. (2013), "Seismic control of power transmission tower using pounding TMD", *J. Eng. Mech.,* **139**(10), 1395-1406. https://doi.org/10.1061/(asce)em.1943-7889.0000576.

Zhang, P., Ren, L., Li, H., Jia, Z. and Jiang, T. (2015), "Control of wind-induced vibration of transmission tower-line system by using a spring pendulum", *Math. Probl. Eng.*, **2015**, 1–10.

https://doi.org/10.1155/2015/671632.

CC